Multiple scaling in a one-dimensional sandpile

V. B. Priezzhev[1] and K. Sneppen[2]
[1]*Laboratory of Theoretical Physics, Joint Institute for Nuclear Research, Dubna 141980, Russia*
[2]*NORDITA, Blegdamsvej 17, DK-2100 Copenhagen, Denmark*
(Received 5 December 1997)

We study the Abelian one-dimensional sandpile model in which the toppling at a site periodically depends on the number of previous topplings at that site with the period T. When T tends to infinity, the redistribution of particles in unstable states becomes completely stochastic. For finite T, we found the probability distribution of avalanche sizes. We show that it is qualitatively similar to a multifractal scaling form obtained earlier for the sandpile model with fixed toppling conditions on decorated one-dimensional chains [A. A. Ali and D. Dhar, Phys. Rev. E **52**, 4804 (1995)]. [S1063-651X(98)04507-3]

PACS number(s): 64.60.Lx, 05.40.+j, 64.60.Ht, 05.70.Ln

The study of dynamics on one-dimensional (1D) chains has revealed a variety of qualitatively new and complex phenomena. This ranges from the early discussion of Anderson localization in random potentials to recent attempts to simplify 3D turbulence to a transport along a 1D chain. Lately, there have been proposed examples of 1D systems that exhibit self-organized criticality (SOC) [1], both with [2–5] and without conservation laws [6–8,5]. In all cases, the 1D systems have proven to be able to sustain an intermittent dynamics, which in the case of most of the SOC models can be well characterized by a single scaling relation in the form of a power law with a finite-size correction .

However, critical behavior of 1D models typically involve some randomness, either in terms of stochastic toppling rules as in the case of critical 1D sandpile models, or in the form of intrinsic chaotic motion as in the 1D train version of the Burridge-Knopoff model [9].

In this work, we study origins of criticality in the 1D sandpile models by considering a sequence of 1D regular models where the random model, here denoted the Manna model, appears as a limit. The 1D version of the Manna model [10,11,5] is equivalent to the rice pile model [3], and thus it belongs to the same universality class [4] as other stochastic SOC models with a conservation law [2,12,9]. Each representative of the sequence of 1D regular models considered here is a pseudorandom model constructed by means of a spiral dynamics introduced in [13], and termed the dynamics of Eulerian walkers (EW). The motion of EW themselves is deterministic. With each site of the lattice one associates an arrow that can point along one of the bonds connecting it with neighboring sites. The arrow directions at a site i are specified by integers n_i $(1 \leqslant n_i \leqslant \tau)$, where τ is the number of nearest neighbors of the site in a given lattice. At each time step, the walker arriving at a site i changes the arrow direction from n_i to $n_i+1 (\mathrm{mod}\ \tau)$ and moves one step from i along the new arrow direction. Thus, the motion of the walker is affected by medium, and in turn affects the medium inducing strong correlations between arrows.

The EW model admits natural generalization along two directions. First, we can introduce waiting time similar to that in the sandpile model: Each walker arriving at a site waits there until the number of particles waiting at that site is $\geqslant r$. Then, these r particles take one step in the directions $n_i+1, n_i+2, \ldots, n_i+r (\mathrm{mod}\ \tau)$ and the arrow is reset to $n_j + r (\mathrm{mod}\ \tau)$. Secondly, we can ascribe to τ nearest neighbors more than τ integers, say $k\tau$ numbers $1,2,\ldots,k\tau$, by k numbers to each, and arrange them in an arbitrary order. If the ratio $T=k\tau/r$ is integer, we obtain a sandpile model with toppling rules that vary periodically with the period T at each site.

This pseudorandom model tends to the random 1D model for large T if integers $1,2,\ldots$ are uniformly distributed among arrow directions at each site in the limit $T \to \infty$. For finite T, the model belongs to the class of Abelian sandpile models (ASM) and some of its properties can be determined exactly. Among them, the most important is the fact that probabilities of all allowed configurations of arrows and occupation numbers are equal in the steady state [14].

We start with a simplest nontrivial 1D case $\tau=2$, $r=2$, $T=3$. Each site contains a counter of topplings that shows the number of the last toppling taken by modulo 3. We ascribe integers 1,2,5 to the left direction and 3,4,6 to the right direction providing the movement of two particles left at each first (mod3) toppling, right at each second (mod3) toppling and in the opposite sides at each 3D (mod3) toppling at the given site. A configuration C of the model is a set of non-negative occupation numbers z_i and the numbers of the last topplings $\mu_i = 1,2,3$ (mod3) assigned to each site of the lattice: $C=\{z_i,\mu_i\}, i=1,2,\ldots,L$. The configuration C is stable if all z_i are below $r=2$. If C is unstable, so that $z_i \geqslant r$ for some i, the site i topples by a rule depending on μ_i and the current value of μ_i increases by 1: $\mu_i \to \mu_i + 1 (\mathrm{mod}3)$.

To describe the transformation resulting from dropping a particle on the site i and allowing the system to evolve, we define the operator a_i acting on the stable configuration C and producing a new stable configuration: $a_i C = C'$. The operators a_i all commute as the operators of arrow rotations and topplings both commute in EW and ASM, respectively. The commutativity rule provides the construction of an Abelian group defined by Dhar [14] for the ASM.

In particular, all recurrent configurations can be obtained from a fixed one by successive acting by operators a_i taken n_i times each

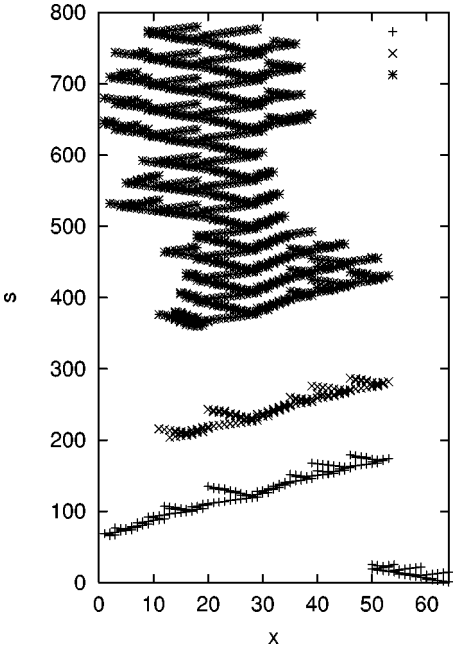

FIG. 1. Response of a system of size $L=64$ and $T=3$ at the recurrent state to excitations at four different places. At the bottom we see the space-time plot of two boundary avalanches initiated at the right and left boundary. Higher in the plot we show linear and respectively massive avalanches arising as a response in the bulk.

$$C=\prod_{i\in L}(a_i)^{n_i}C^*. \tag{1}$$

Thus, any recurrent configuration can be represented by an L-dimensional vector $\{n_1,n_2,\ldots,n_L\}$. Among different vectors, however, there are equivalent ones. The identity operator has the form

$$E_i=\prod_{j\in L} a_j^{3\Delta_{ij}}, \tag{2}$$

where $\Delta_{i,j}$ is the Laplacian matrix with elements $\Delta_{i,j}=2$ if $i=j$, $\Delta_{i,j}=-1$ if i and j are connected by a bond and $\Delta_{i,j}=0$ otherwise. Equation (2) follows from observation that two procedures produce the same effect: (i) a_i^6—adding 6 particles at a given site and allowing them to evolve to a stable configuration; (ii) $a_{i-1}^3 a_{i+1}^3$—adding 3 particles at the nearest neighbors of i. The identity operator allows one to find the total number of nonequivalent vectors by identification of an elementary cell in the L-dimensional space. Then, the number of all possible recurrent configurations is the volume of the elementary cell

$$N=3^L\det\Delta=3^L(L+1). \tag{3}$$

The entropy per site is equal to ln(3) in the large L limit in contrast with the simple 1D sandpile where entropy per site is zero in the recurrent state. The nonzero value of entropy opens for nontrivial dynamical behavior of the model.

In Fig. 1 we show the response of the system to adding a grain at different positions of the lattice. The response is widely different: in the case we add a particle to a boundary site, left or right, an excitation traverses the system in a solitonlike manner when localized instability propagates along the lattice with a constant velocity. As a result, all sites involved into the relaxation topple exactly 3 times, except maybe a finite number of sites at the initial and final stages of the process. In the second case, particles added in the bulk induce a diversity of avalanche shapes including large compact avalanches.

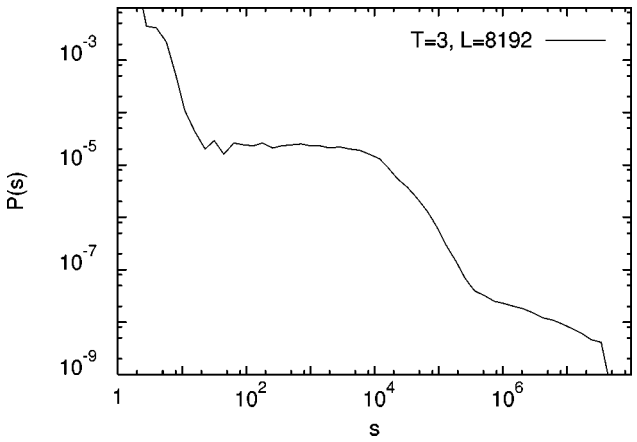

FIG. 2. Probability of avalanche size counted as the number of topplings in the recurrent state. The toppling rules used had $T=3$ and the system size was $L=8192$.

In Fig. 2 we show the distribution of avalanche sizes obtained at steady state conditions. We notice two scaling regimes, one regime with $P(s)\sim 1/s^0$ valid for avalanches with the number of topplings between size of an order of 10 and the system size L. The second regime spreads from avalanche sizes of the order of $L^{3/2}$ until L^2 where finite size effects become essential. For these large avalanches we observe $P(s)\sim 1/s^{1/2}$. Closer inspection of the avalanches of the first regime reveals that these mostly look like the boundary avalanches where each site inside the avalanche topples 3 times.

The analysis of the avalanche structure may be simplified by using ''waves of toppling'' introduced in [16]. Due to the Abelian property of the model, we can topple unstable sites in an arbitrary order. We choose the following one: add a particle to the site i having the height $r-1$ and topple all unstable sites until they are stable except the source site i, which is allowed to topple not more than 3 times. This sequence of topplings is called the first wave of topplings. After the first wave has gone out, and the site i is still unstable, we continue the avalanche, not permitting this site to topple more than 3 more times. The set of relaxed sites in the period after the first wave is the second wave. This process continues until the whole lattice becomes stable.

It is easy to deduce that any site covered by a wave topples during the wave not more than 3 times. Indeed, to topple a site j more than 3 times, one of the sites $j+1$ or $j-1$ should be toppled more than 3 times first. From this, one of the sites $j+2$ or $j-2$ should be toppled more than 3 times. Continuing, we reach the initial point i of the wave, which is toppled once. Therefore, none of the sites involved into the wave topples more than 3 times.

The propagation of waves from the open boundaries is of special interest. Let us add 3 particles to the left boundary site $i=1$ and to the right boundary site $i=L$. Using the identity

$$a_1^3 a_L^3 = a_0^3 \left(\prod_{i=1}^{L} E_i^{-1} \right) a_{L+1}^3 \tag{4}$$

we see that the operator $a_1^3 a_L^3$ ensures the transfer of 3 particles from the left edge to the site $i=0$ and from the right edge to the site $i=L+1$. The occupation numbers of all lattice sites $i=1,2,\ldots,L$ remain unchanged. The only possibility to realize this procedure is the uniform three-fold toppling of all lattice sites. This gives a useful algorithm to verify if a given configuration C is the recurrent one: C is recurrent if all sites of the lattice topple exactly 3 times after adding 3 particles to both the boundary sites; C is forbidden in the recurrent set if a subset of the lattice topples less than 3 times.

We can also deduce that the waves are compact with respect to maximal topplings: if the sites i and j $(i<j)$ topple 3 times during the wave, the sites $i+1,i+2,\ldots,j-1$ topple also 3 times. Otherwise, the given configuration contains a forbidden subconfiguration.

If we add 3 particles only to the left boundary site $i=1$ of the recurrent configuration C, we generate the left boundary wave propagating from the edge to a site j, $1 \leqslant j \leqslant L$, which topples $n<3$ times. The wave initiated at the opposite edge reaches this point and topples it $3-n$ times providing the uniform three-fold toppling of the whole lattice. We refer to such a site as the break point (BP). By definition, the BP is unique. The examples of the waves propagating from the left and right edges are shown in Fig. 1. Connecting all points corresponding to topplings whose time and space coordinates differ by 1, we obtain a phase portrait of the left boundary wave. The left boundary wave together with the right one gives a graph representation of the recurrent configuration C. Particular values of z_i and μ_i at any site i can be recovered in a unique way from the local structure of the graph in the vicinity of the point i. The one-dimensional structure of the graph testifies to the exponential decay of correlations and lack of the self-organized criticality in our model.

The main objective of the wave analysis is to show that there exist three types of avalanches: short (class N), linear (L) and massive (M). We start with a simple but essential proposition. Given a recurrent configuration C consider an avalanche triggered at the site $i, 1 \leqslant i \leqslant L$. Suppose the site i topples at least 3 times during the avalanche. Then, the avalanche reaches the BP. To prove this, consider the interval (i,j) between the starting point i and the point j where the BP is located. Assume $i \leqslant j$ for definiteness. The left boundary wave covers the interval (i,j) by the definition of the BP. During the course of the left wave, the point i topples 3 times, transferring 3 particles inside the interval (i,j) in a certain order depending on the value of μ_i in C. Consider an avalanche initiated at i and exhibiting at least 3 topplings. The first 3 topplings of the avalanche lead to the transfer of 3 particles inside (i,j) exactly in the same order as 3 topplings of the left boundary wave. Therefore, the avalanche propagates up to the BP. Similarly, we can prove that if the toppling process triggered at the site i causes three-fold toppling at a site $i', i \leqslant i' \leqslant j$, the avalanche reaches the BP as well.

The proven statement allows us to select the first type of avalanche. We will say an avalanche belongs to the class N (the normal one) if it causes fewer than 3 topplings in any point of the interval between the initial point and the BP and thus does not necessarily reach the BP. It is clear that the restriction on the number of topplings leads to a restriction on the total mass of avalanches. These small avalanches are responsible for the initial part of the distribution $P(s)$ shown in Fig. 2. When the period $T \to \infty$ the restriction is lifted the avalanches of class N form the single scaling relation of the Manna model.

Consider the case when at least one site between the initial point and the BP undergoes more than 3 topplings. Then, the avalanches propagate up to the BP no matter how far it is located. If, in the process, the avalanche does not spread significantly on the other side of the initiation point, it has a linear structure and belongs to the class L of linear avalanches. The avalanches of the class L can be decomposed into a finite number of waves having the length of an order of $j-i$ each. The first wave moves towards the BP at the site j with a finite average velocity that depends on mean values of the occupation numbers z_k and the fraction numbers of sites having given values of $\mu_k=1,2,3$. As the sites inside the wave topple 3 times each, the initial configuration remains unchanged there. Therefore, next waves repeat the motion of the first wave everywhere except the initial and final stages. The total number of topplings in the avalanche is

$$s \sim 3 m_i (i - i'), \tag{5}$$

where i and i' are the positions of the source point and BP on the chain and m_i is the number of periods at the site i. Since the avalanche spreads a finite distance to the left, m_i is finite and $s \sim L$. The value of m_i depends on the specific arrangement of numbers z_i, μ_i in a cluster of sites in the vicinity of the source point. Due to translation invariance, the positions of the source point and the BP are uniformly distributed on the lattice. This implies that the avalanches of the class L are distributed as

$$P(s) \sim \frac{1}{L} f_1 \left(\frac{s}{L} \right), \tag{6}$$

where f_1 is a nonuniversal function that is constant for small arguments.

The uniform distribution of wave sizes can be derived in a more regular way. Each site j of the lattice involved in an avalanche initiated at the site i is characterized by the total number of topplings M_{ij} during the avalanche and by the number of periods of topplings T_{ij} where $T_{ij} \geqslant 0$ is the maximal integer less than $M_{ij}/3$. It follows from dynamical rules that the expected value of $\overline{T_{ij}} = G_{ij}$ is maximal at the site where the avalanche has been initiated and monotonically decreases with distance from this site. Indeed, the expected number of particles leaving the site j is $3\Delta_{jj} G_{ij}$ whereas $-3\Sigma_{k \neq j} G_{ik} \Delta_{kj}$ is the average flux into j. Equating both the fluxes one gets

$$\sum_k G_{ik} \Delta_{kj} = \delta_{ij}. \tag{7}$$

The Green function $G_{ij} = [\Delta^{-1}]_{ij}$ in the 1D case is a linear decreasing function of the distance $|i-j|$ if both i and j are situated deeply inside the interval $[0,L]$. Since a wave is the

compact set of three-fold topplings, G_{ij} coincides with the distribution function of waves whose linear extent exceeds $|i-j|$. The linear dependence of G_{ij} on $|i-j|$ leads to the uniform distribution of wave sizes.

The third class is formed by avalanches that spread a distance $O(L)$ on both the sides of the source point. Again, we can decompose the avalanche into waves, but in this case, the propagation of waves is qualitatively different for different directions. The motion of the first wave to the right is the same as for the class L. The front of the wave moves with a fixed average velocity and stops at the BP.

The motion of the left front is less regular. The first left wave moves up to a first obstacle when no more topplings are possible. The second wave can overflow the stop point or, vice versa, step back several sites. The left front of the next waves behaves similarly, performing a random walk at distances of the order of $L^{\beta}, \beta<1$. Eventually, it reaches the source point i after m_i steps (waves) and the avalanche stops. The probability distribution of the random walks returning to the origin for the first time is [17]

$$P(m_i)\sim \frac{1}{m_i^{3/2}}, \tag{8}$$

which when combined with Eq. (5) gives the leading asymptotics of the distribution $P(s)$ for this kind of avalanches

$$P(s)\sim \frac{1}{L}\,\frac{1}{(s/L)^{3/2}}. \tag{9}$$

It should be noted that one can represent the left front as a simple random walk only approximately. Actually, the correlations between different parts of the front exist. Moreover, the correlation length grows with the period T and tends to infinity for the Manna model due to its criticality. This explains why the law (9) becomes increasingly poor when T grows at a fixed L.

At distances of an order of L, the left front of the sequence of waves moves as a biased random walk. It drifts from the source point toward the left boundary with a constant average velocity. The important property of the constant front velocity can be derived from the uniform distribution of wave sizes connected with linearity of the Green function G_{ij}. To see this, consider an interval Δl of the lattice situated at the distance l from the initiation point i. Let m waves propagating from i stop in this interval. The average velocity of the avalanche front is proportional to the density of stops in Δl. But the uniform distribution of wave sizes implies the uniform distribution of stops. Therefore, the average velocity of the front does not depend on the distance l from the source point.

The behavior of the right front after reaching the BP is different for two cases: (i) consequent waves cross the BP and the front drifts to the right boundary; (ii) the front reflects from the BP and moves back to the source point.

When the front reaches the boundary, left or right, it reflects and moves in the opposite direction with a constant average velocity. When two backward fronts or one backward and one direct fronts meet, the avalanche stops. The avalanches spreading to both directions a distance $O(L)$ and returning back with a constant velocity scale as L^2 and should be referred to the third class M (massive avalanches). The total number of topplings in these avalanches depends on the positions of the initiation point and the BP. Each of them occupies one of the L positions on the lattice; so the probability of a given size s is proportional to L^{-2}. Thus, we can write the size distribution for avalanches of the class M in the form

$$P(s)\sim \frac{1}{L^2} f_2\left(\frac{s}{L^2}\right), \tag{10}$$

where f_2 is a nonuniversal function.

Now, we may characterize the scaling behavior of avalanches with the multifractal formalism [18]. For large L, the distribution of avalanches of sizes $s\sim L^{\alpha}$ scales as $L^{f(\alpha)}$ where the multifractal exponent $f(\alpha)$ is given by [18]

$$f(\alpha)=\lim_{L\to\infty} \ln[\mathrm{Prob}_L(s=L^{\alpha})]/\ln(L) \tag{11}$$

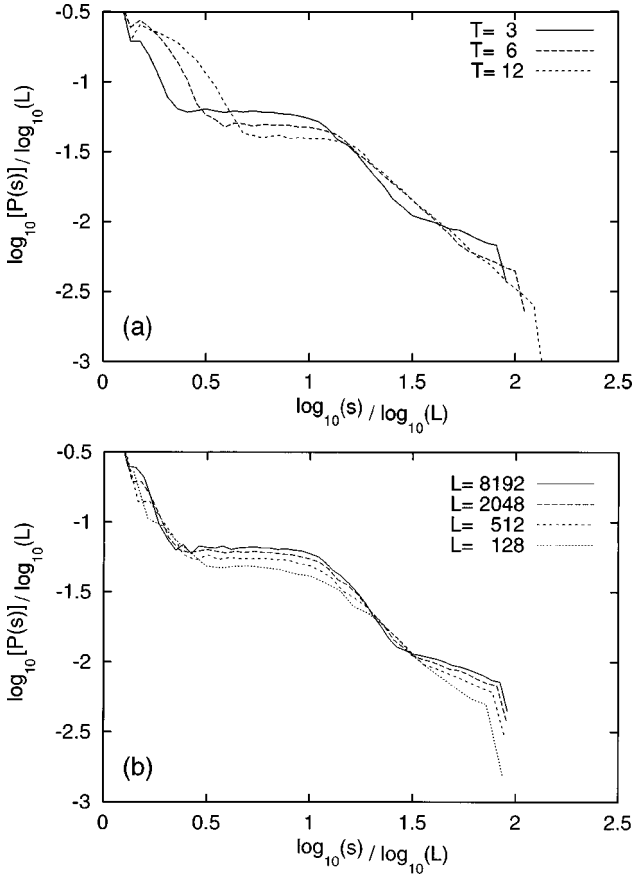

FIG. 3. (a) Rescaled avalanche distributions for different toppling periods $T=3,6,12$. In all cases we considered system size $L=2048$. We observe that the crossover between different regimes moves slightly with the period approaching the single scaling form (15). (b) Avalanche distributions plotted as in (a), but here for 4 different system sizes, $L=128,512,2048,8192$ and $T=3$. One observes the two scaling regimes, for linear and massive avalanches, plus some regime for small avalanches. In all cases the contribution of small avalanches stops at $s\sim L^{0.3\pm0.05}$, the scaling of linear avalanches stops at $s\sim L$, and the cutoff for the largest avalanches scales as $s\sim L^{2.10\pm0.05}$.

Ali and Dhar [15] have found the multifractality in 1D ASM on decorated chains formed by joining doublets or diamonds. They have demonstrated that the distribution function is a linear combination of two scaling forms

$$\mathrm{Prob}_L(s)=L^{-1}f_1(s/L)+L^{-2}f_2(s/L^2), \tag{12}$$

where f_1 and f_2 are nonuniversal scaling functions. They found a subclass of avalanches whose distribution is singular at small s/L^2. The diverging contribution comes from avalanches having a form of polygons with the linear size of an order of the distance R between the source point and BP. In this case $s\sim R^2$ and $\mathrm{Prob}(R)\sim$const. Therefore, the function $f_2(s/L^2)$ contains the square-root singularity

$$f_2(s/L^2)\sim\left(\frac{L^2}{s}\right)^{1/2} \tag{13}$$

for $s\to 0$. In our model, this subclass of avalanches belongs to the class M.

From Eqs. (6), (9), (10), and (13), we have

$$f(x)=\begin{cases} -1 & \text{if } \alpha_0\leqslant\alpha\leqslant 1 \\ \frac{1}{2}-\frac{3}{2}\alpha & \text{if } 1\leqslant\alpha\leqslant\frac{3}{2} \\ -1-\frac{1}{2}\alpha & \text{if } \frac{3}{2}\leqslant\alpha\leqslant 2 \end{cases}. \tag{14}$$

The numerical value of the lower bound $\alpha_0\approx 0.3$ is conditioned by the scaling behavior of the large avalanches belonging to the class N in the limit $L\to\infty$.

Our consideration may be easily generalized to an arbitrary period T. In spite of growing fluctuations, the main conclusion about the constant average velocity of wave fronts remains true. The limiting form of the avalanche sizes distribution $P(s)$ depends on the order one takes the $L\to\infty$ then $T\to\infty$. The first case is illustrated by Fig. 3(a). We see that the horizontal segment reduces and sinks when T grows at a fixed L and the right edge elongates and sinks too. As a result, the contribution from the class N grows and we can expect $f(\alpha)$ approaches to a single function corresponding to the scaling form

$$\mathrm{Prob}(s)\sim\frac{1}{s^\tau}f_s\left(\frac{s}{L^2}\right), \tag{15}$$

where $\tau\approx 1.1$ is the critical exponent of the Manna model and $D\approx 2.2$ is the avalanche dimension. Thus, the normal avalanches dominate both the linear and massive avalanches.

More interesting, however, is the opposite order of limits. This case is shown in Fig. 3(b). Fixing T, we consider lattices of growing sizes. Then the horizontal segment rises tending to the value -1 and the right edge tends to the point $(-2,2)$ in the limit $L\to\infty$ in accordance with Eq. (14). Varying T, we find that the points $(-1,1)$ and $(-2,2)$ are the fixed points of the period transformation. When $T\to\infty$ after $L\to\infty$, the bound α_0 determining the contribution of the class N avalanches goes right. The limiting value of α_0 is an interesting open problem. If α_0 approaches the point $(-1,1)$, the slope of $f(\alpha)$ in the interval $0\leqslant\alpha\leqslant 1$ is 1, which corresponds to $\tau=1$ and $D=2$ in the Manna model. However, if $\tau>1$ for the limiting slope of $f(\alpha)$ on the interval $0\leqslant\alpha\leqslant\alpha_0$, then α_0 approaches the limit $\alpha_0=1/\tau$ and the horizontal segment of $\ln P(s)$ has to survive even for large lattices and large periods.

In summary, we have studied deexcitation of a deterministic 1D sandpile model decorated with phase ordered toppling rules. The model exhibits widely different avalanche responses to perturbation: linear wavelike avalanches and massive polygonlike avalanches. Apart from these two responses there are avalanches of traditional SOC models. As the toppling period extends, the scaling of the SOC avalanches extends to dominate both the linear and the massive avalanches. We find it interesting that phase ordering of deexcitation in 1D may give such a diversity of phenomena.

This work was supported by the Russian Foundation for Fundamental Research through Grant No. 97-01-01030. V.B.P. thanks NORDITA for its hospitality.

[1] P. Bak, C. Tang, and K. Wiesenfeld, Phys. Rev. Lett. **59**, 381 (1987).
[2] S. I. Zaitsev, Physica A **189**, 411 (1992).
[3] V. Frette, K. Christensen, A. Malte-Sørensen, J. Feder, T. Jøssang, and P. Meakin, Nature (London) **379**, 49 (1996).
[4] M. Paczuski and S. Boettcher, Phys. Rev. Lett. **77**, 111 (1996).
[5] H. Nakanishi and K. Sneppen, Phys. Rev. E **55**, 4012 (1997).
[6] K. Sneppen, Phys. Rev. Lett. **69**, 3539 (1992).
[7] P. Bak and K. Sneppen, Phys. Rev. Lett. **71**, 4083 (1993).
[8] M. Paczuski, S. Maslov, and P. Bak, Phys. Rev. E **53**, 414 (1996).
[9] M. de Sousa Vieira, Phys. Rev. A **46**, 6288 (1992).
[10] S. S. Manna, J. Phys. A **24**, L363 (1991).
[11] A. Ben-Hur and O. Biham, Phys. Rev. E **53**, R1317 (1996).
[12] Y.-C. Zhang, Phys. Rev. Lett. **63**, 470 (1989).
[13] V. B. Priezzhev, D. Dhar, A. Dhar, and S. Krishnamurthy, Phys. Rev. Lett. **77**, 5079 (1996).
[14] D. Dhar, Phys. Rev. Lett. **64**, 1613 (1990).
[15] A. A. Ali and D. Dhar, Phys. Rev. E **52**, 4804 (1995).
[16] E. V. Ivashkevich, D. V. Ktitarev, and V. B. Priezzhev, J. Phys. A **27**, L585 (1994).
[17] W. Feller, *An Introduction to Probability Theory and Its Applications*, Vol. 1 (John Wiley, New York, 1950).
[18] L. P. Kadanoff, S. R. Nagel, L. Wu, and S. Zhou, Phys. Rev. A **399**, 6524 (1989).